

Efficient Creation and Morphological Analysis of ABC Triblock Terpolymer Libraries

Elizabeth A. Murphy, Yan-Qiao Chen, Kaitlin Albanese, Jacob R. Blankenship, Allison Abdilla, Morgan W. Bates,* Cheng Zhang,* Christopher M. Bates,* and Craig J. Hawker*



Cite This: <https://doi.org/10.1021/acs.macromol.2c01480>



Read Online

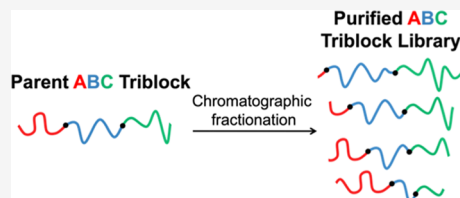
ACCESS |

Metrics & More

Article Recommendations

Supporting Information

ABSTRACT: Multiblock copolymers with increasingly complex block sequences—for example, triblock terpolymers—offer unique opportunities to create nanostructured materials, but this potential has been hindered by a vast design space that complicates the exploration of structure–property relationships. Here, we report a versatile and scalable strategy to separate parent ABC and isomeric ACB triblock terpolymers into libraries of fractionated samples spanning a wide range of compositions. Using a combination of controlled polymerization and automated chromatography, the synthesis and separation of less than 10 ABC and ACB parent materials gave rise to over 100 purified triblock terpolymers. Separations follow systematic and predictable trends in volume fraction resulting from an adsorption-based mechanism where chains rich in non-polar blocks elute first, followed by more polar derivatives, yielding fractions with improved purity in composition and molar-mass dispersity. As evidenced by small-angle X-ray scattering, fractionation significantly enhances long-range order compared to as-synthesized parent materials and allows for the definitive identification of various nanoscale morphologies. This user-friendly separation strategy significantly increases the availability of well-defined ABC triblock terpolymer libraries to the polymer community while also improving sample quality and accelerating discovery.



INTRODUCTION

Block copolymers have received considerable attention as materials that self-assemble into a rich array of nanoscale morphologies with applications ranging from advanced microelectronics to nanomedicine delivery systems.^{1–4} The simplest sequence, an AB diblock copolymer, has been extensively studied by a synergistic combination of experiments and simulations,^{5–7} which have provided a comprehensive understanding of basic phase behavior. In contrast, as the number of blocks (n) and block types (k) grows even modestly, an exponential increase in synthetically tunable parameters renders the situation considerably more complex.⁸ Primary factors that control equilibrium phase behavior include block volume fractions f_i (where $i = 1, 2, \dots, n$), degrees of polymerization (N_i), Flory–Huggins interaction parameters (χ_{ij} , $i \neq j$), and statistical segment lengths b_i . More recently, secondary structural characteristics such as polymer sequence, architecture, and dispersity (in both molar mass and composition) have also been shown to influence morphology.^{9–11} This long list of structural features illustrates the difficulty in navigating and controlling a multidimensional design space. Advances in both experiments and theory for multiblock copolymers are therefore rate-limited by the effort associated with traditional serial synthetic strategies and/or performing large numbers of simulations (even those subject to the mean-field approximation, for example, self-consistent field theory, “SCFT”). Furthermore, conventional synthetic approaches suffer from inevitable difficulties in matching block

molecular weights between different samples and minimizing homopolymer or diblock copolymer impurities.

Although a comprehensive picture of multiblock copolymer phase behavior has yet to emerge, advances in controlled polymerization techniques are making these complex sequences more readily accessible. For example, Anastasaki reported the synthesis of decablock copolymers with concurrent control over sequence and dispersity using a switchable reversible addition–fragmentation chain transfer (RAFT) agent generated *in situ*.¹² In a similar vein, Haddleton described the synthesis of sequence-controlled multiblock polymers containing up to 21 blocks via sulfur-free RAFT emulsion polymerization,^{13,14} while our group has demonstrated the synthesis of ABCDE multiblock copolymers with hydrophobic, hydrophilic, and semifluorinated segments through light-mediated atom-transfer radical polymerization.¹⁵ Despite these synthetic advances, the application of controlled polymerization strategies to systematically explore multiblock copolymer phase space remains challenging.

In an effort to accelerate the study of block copolymer phase behavior, we recently described the use of automated

Received: July 17, 2022

Revised: September 15, 2022

chromatography to purify a single, as-synthesized AB diblock copolymer into individual fractions spanning a wide range of compositions (f_A). This user-friendly chromatography technique facilitated the rapid generation of linear AB diblock copolymer libraries and significantly simplifies the exploration of block copolymer phase space.^{16,17} Other research groups have also used this strategy to fractionate low-molecular-weight homopolymers into discrete oligomers for a variety of applications.^{18–35} Notably, the combination of controlled polymerization and automated chromatography has not been applied to more complex sequences of blocks, even though the potential for accelerated discovery is amplified. Work by Williams demonstrated the separation of poly(styrene)-block-poly(*tert*-butyl acrylate)-block-poly(methyl methacrylate) linear triblock terpolymers through thermal field-flow fractionation (ThFFF).³⁶ However, this technique is not readily scalable (<100 mg) and requires a careful balance between sample/solvent compatibility and multiple detectors.

Here, we apply a much simpler automated chromatography strategy to the separation of ABC and isomeric ACB triblock terpolymers. Significantly, this approach is scalable and utilizes standard laboratory equipment, which makes it accessible to researchers with diverse expertise. As a result, only a limited number of parent triblock terpolymers need be prepared and subsequently purified to generate a wide range of terpolymers, which eases the synthetic burden associated with exploring phase space. These advantages are particularly acute in the context of ABC triblock terpolymers, where a substantial body of prior work has investigated phase behavior by uniquely synthesizing each triblock sample. To illustrate this challenge, Epps^{37–39} investigated the phase behavior of poly(isoprene)-block-poly(styrene)-block-poly(ethylene oxide) by synthesizing 44 individual ABC triblock terpolymers by anionic polymerization. In a similar serial fashion, poly(styrene)-block-poly(butadiene)-block-poly(2-vinylpyridine)^{9,40,41} and poly(styrene)-block-poly(butadiene)-block-poly(methyl methacrylate)⁴² ABC triblock terpolymers were studied by Abetz and Stadler with over 50 triblocks prepared anionically. Significantly, each anionic polymerization requires the rigorous purification of reagents, an understanding of reaction kinetics for accurate timing of sequential block additions, and multiple isolation steps, greatly increasing the time and cost of material synthesis. In contrast, here, we report the generation of over 100 purified, narrow-dispersity, and well-ordered triblock terpolymers from just 8 as-synthesized samples. These results highlight the power of combining controlled polymerization procedures with automated chromatography to accelerate the study of block copolymer phase behavior, especially for materials having more sequence complexity than the prototypical AB diblock (Figure 1). The versatility of this approach is further illustrated by the facile synthesis, purification, and study of a corresponding isomeric ACB triblock terpolymer system.

RESULTS AND DISCUSSION

The design of ABC triblock terpolymers for this study based on A = poly(4-methyl caprolactone) (L), B = poly(dodecyl acrylate) (D), and C = poly(2,2,2-trifluoroethyl acrylate) (F) was governed by three primary criteria. First, the blocks have large differences in polarity (L: more polar; D: less polar; F: fluorinated) which we hypothesized would lead to efficient fractionation via an adsorption-based mechanism at high molecular weights.¹⁶ Second, all the thermal transitions lie

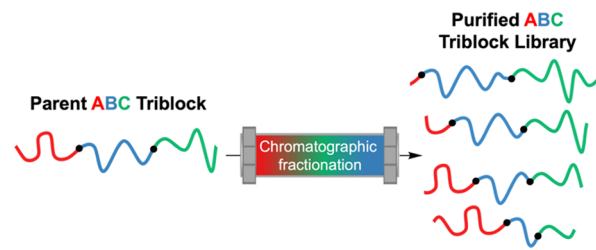


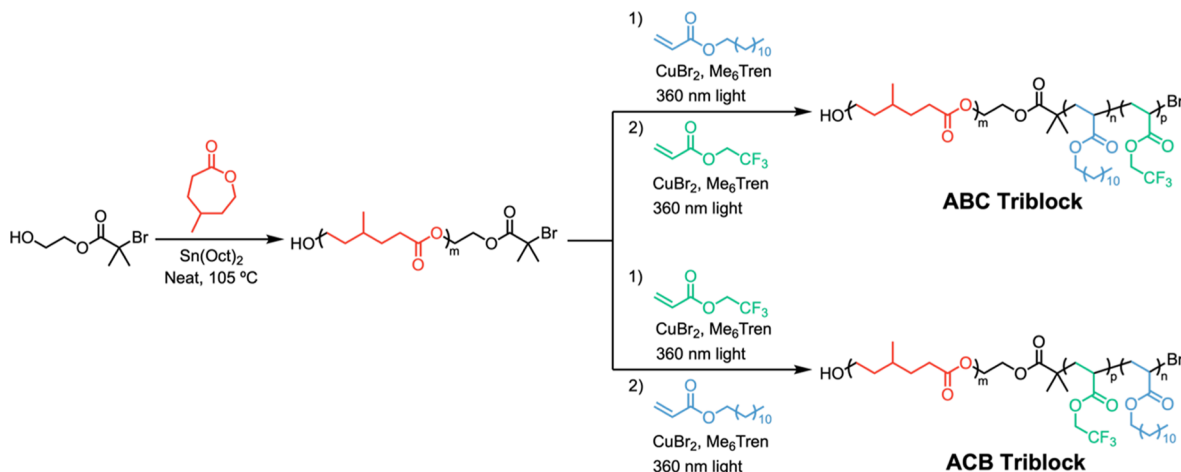
Figure 1. Automated chromatographic separation of an ABC triblock terpolymer generates a well-defined library of fractionated samples spanning a wide range of volume fractions.

below room temperature ($T_{g,L} = -60^\circ\text{C}$, $T_{m,D} = 0^\circ\text{C}$, $T_{g,F} = 1^\circ\text{C}$), which facilitates thermal annealing under mild conditions.^{43,44} Third, each interaction parameter (χ_{ij}) is high as evidenced by small-angle X-ray scattering (SAXS) experiments conducted on the three different diblock pairs (Figures S18–S20). Self-assembled structures will therefore be stable at accessible molecular weights, minimizing kinetic effects that may interfere with morphological analysis.

Based on the target ABC triblock terpolymer chemistry, syntheses were conducted via sequential ring-opening polymerization (ROP) and photo-initiated atom-transfer radical polymerization (ATRP) from an orthogonal difunctional initiator, 2-hydroxyethyl 2-bromo isobutyrate (HEBiB) (Scheme 1). Compared with traditional anionic strategies, an advantage of this approach is the ability to store and fully characterize precursor homopolymers and diblock copolymers before synthesizing the final triblock terpolymer. Consequently, a single large batch of poly(4-methyl caprolactone) homopolymer was synthesized through ROP catalyzed by tin(II) 2-ethylhexanoate ($\text{Sn}(\text{Oct})_2$) with full characterization prior to sequential chain extension with dodecyl acrylate followed by 2,2,2-trifluoroethyl acrylate under photo-ATRP conditions using an aliphatic tertiary amine ligand (Me_6Tren) and low concentrations of copper(II) bromide (CuBr_2) with UV irradiation (360 nm light). The orthogonality of ROP and ATRP, coupled with high end group retention for each step, enabled the preparation of well-defined ABC triblock terpolymers in high yields.

Characterization of the ABC triblock copolymers was facilitated by unique ^1H NMR resonances for each block. This is illustrated in Figure 2, where the resonance for the CH_2O group of 4-methylcaprolactone (labeled h) is observed at ~ 4.1 ppm, in contrast to dodecyl acrylate (resonance i) at ~ 4.0 ppm and 2,2,2-trifluoroethyl acrylate (resonance k) at ~ 4.5 ppm. Integration of these peaks compared to one from the initiator fragment (labeled a) allowed for an accurate calculation of the molecular weight and volume fraction of each block. These results combined with the shift in size-exclusion chromatograms to lower elution times upon chain-extending poly(4-methylcaprolactone) homopolymer to the corresponding AB and ABC block copolymers demonstrate good control over the synthesis of these materials in high yield (Figure S8).^{15,45,46} To highlight the versatility of this triblock system, we synthesized five parent ABC triblock terpolymers with different volume fractions (Table S1). For each parent terpolymer, sufficient molecular weights were targeted to ensure that all three blocks microphase separate (Figures S18–S20). Note that our sample nomenclature reflects the order of block connectivity (LDF), places $f_L \times 100$ after the dash (LDF-22), and uses angle

Scheme 1. Synthesis of ABC and ACB Triblock Terpolymers with Poly(4-methyl caprolactone), Poly(dodecyl acrylate), and Poly(2,2,2-trifluoroethyl acrylate) Blocks Through Sequential ROP and ATRP^a



^aThe sequential polymerization of dodecyl acrylate and 2,2,2-trifluoroethyl acrylate was reversed when preparing isomeric ACB triblock terpolymers.

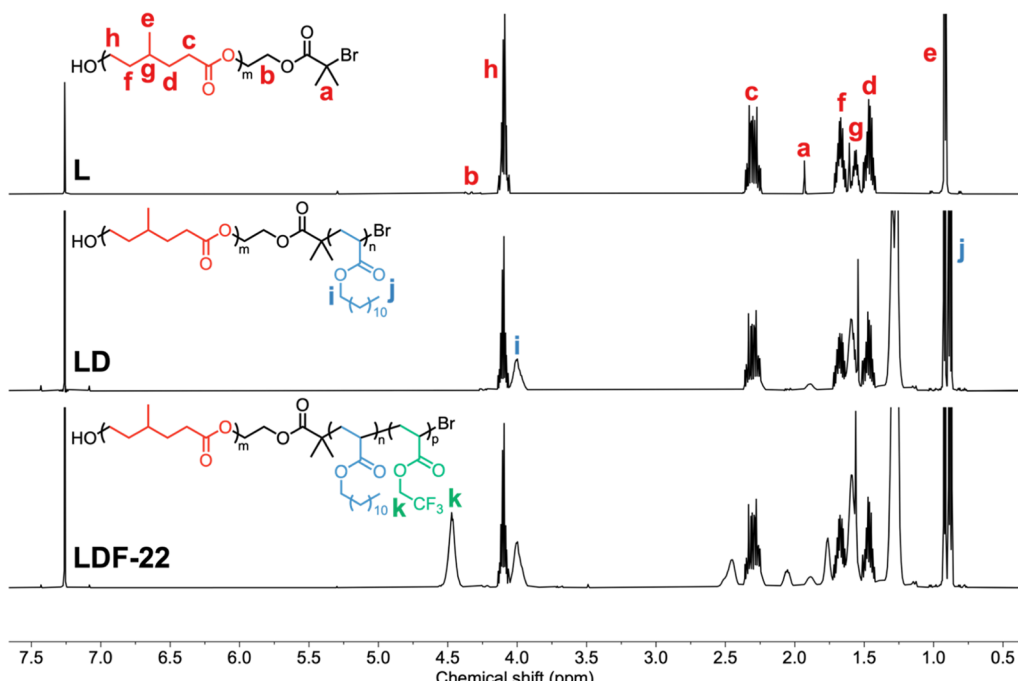


Figure 2. ^1H NMR spectra of the starting poly(4-methylcaprolactone) homopolymer (L), diblock copolymer (LD), and triblock terpolymer (LDF-22) exhibiting unique resonances for all three blocks and the initiator fragment.

brackets $\langle \dots \rangle$ to denote characteristics of the parent triblock copolymers (i.e., before fractionation).

To demonstrate the utility of automated chromatography for preparing a diverse polymer library from a limited number of ABC triblock terpolymers, 1.5 g of a parent LDF triblock terpolymer (LDF-22) with $\langle M_n \rangle = 40 \text{ kg/mol}$, $\langle D \rangle = 1.13$, and initial volume fractions of each block $\langle f_L \rangle = 22\%$, $\langle f_D \rangle = 47\%$, and $\langle f_F \rangle = 31\%$ (Table S1) was dissolved in dichloromethane and loaded directly onto a commercially available (100 g) silica gel column. Importantly, wet loading is significantly preferred over dry loading to ensure solubility of high-molecular-weight species throughout the fractionation. Suitable elution conditions were identified through a series of simple thin-layer chromatography (TLC) experiments (Figure S14). For LDF-

22, an optimized gradient from 100% dichloromethane to 40 vol % ethyl acetate in dichloromethane (25 column volumes) was used to purify and fractionate the parent triblock terpolymer (Table S2, Figure S15).

Using evaporative light scattering detection for each fraction, an initial LDF-22 library of ~90 fractions was appropriately combined to give 30 purified ABC triblock terpolymer samples (30–60 mg each, Figure 3a, Table S3). Significantly, an overall mass recovery of 90% was achieved for this multi-gram-scale separation. In addition, automated chromatography allows for homopolymer and diblock copolymer impurities to be easily identified and removed due to their elution at the beginning of the fractionation process.¹⁶ This enables increased sample purity and reproducibility among fractionated ABC triblock

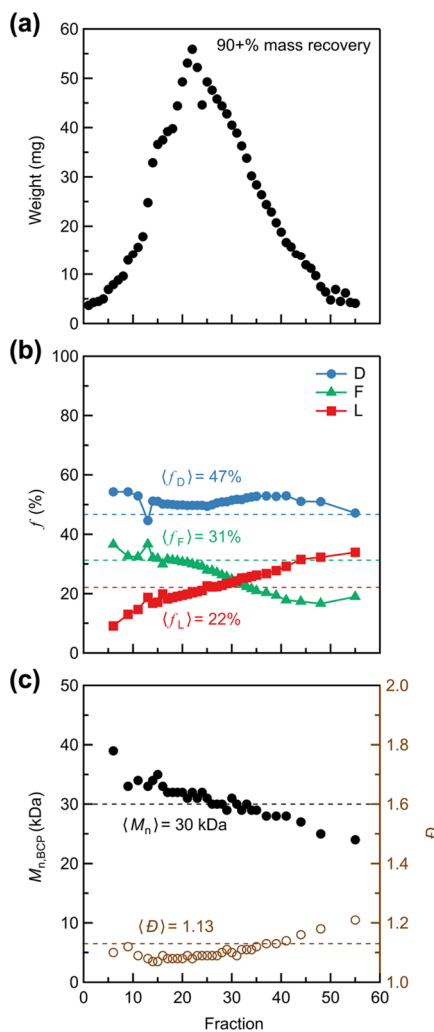


Figure 3. Chromatographic separation of poly(4-methyl caprolactone)-block-poly(dodecyl acrylate)-block-poly(2,2,2-trifluoroethyl acrylate) ABC triblock terpolymer, LDF-22, generates a diverse library of fractionated triblock samples. (a) Mass distribution of collected fractions indicates a high mass recovery of ~90%. (b) Variation of block compositions with f_L increasing and f_F decreasing as the fractionation progresses. Dashed lines represent block volume fractions of the parent triblock terpolymer before fractionation: $\langle f_L \rangle = 22\%$, $\langle f_D \rangle = 47\%$, and $\langle f_F \rangle = 31\%$. (c) Number-average molecular weight and molar-mass dispersity \mathcal{D} of the fractions as determined by SEC (relative to linear polystyrene standards). Dashed lines represent $\langle M_n \rangle$ and $\langle \mathcal{D} \rangle$ of the parent triblock terpolymer before fractionation.

terpolymer libraries. The unique ^1H NMR resonances for each block provide a detailed picture of terpolymer compositional variation across the elution profile as summarized in Figure 3b. Notably, the volume fraction of poly(4-methylcaprolactone), f_L , gradually increases ($9 \rightarrow 47\%$) concomitantly with the decreasing volume fraction of poly(2,2,2-trifluoroethyl acrylate), f_F ($37 \rightarrow 17\%$). In direct contrast, the volume fraction of poly(dodecyl acrylate), f_D , is approximately constant across the library (~50%). Furthermore, size-exclusion chromatography (SEC) shows that the majority of fractionated samples have a lower dispersity ($\mathcal{D} = 1.07\text{--}1.12$) than the parent material ($\langle \mathcal{D} \rangle = 1.13$) (Figure 3c) with a modest decrease in molecular weight as the fractionation progressed. The latter observation is likely due to the poly(2,2,2-trifluoroethyl acrylate) block in the parent material having the highest $\langle M_n \rangle$ and a decreasing

volume fraction throughout the fractionation, with separation being driven by adsorption of polar blocks and not size-exclusion effects.¹⁶ Collectively, these results demonstrate the efficacy and scalability of automated chromatography in generating a high-purity and diverse ABC triblock terpolymer library from a single parent terpolymer.

Having obtained a fractionated library of well-defined and purified ABC triblock terpolymers from the parent (LDF-22), we next investigated their phase behavior using SAXS. Notably, a significant number of the fractionated samples show different morphologies relative to each other as well as the parent terpolymer. In addition, a noticeable increase in the number of peaks was observed upon fractionation, even though a laboratory source instrument was used in all cases. This enhanced long-range order is attributed to the increased purity of fractions. To illustrate the marked difference between a parent and select fractions, Figure 4 shows three scattering

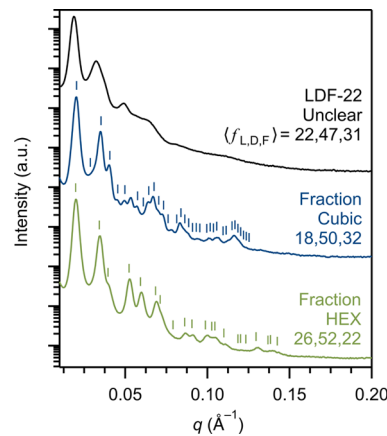


Figure 4. Selected SAXS profiles of a parent ABC triblock terpolymer, LDF-22, and fractions derived therefrom. All SAXS experiments were conducted at room temperature. Triblock terpolymers were annealed at $130\text{ }^\circ\text{C}$ for 15 h and then $70\text{ }^\circ\text{C}$ for 24 h under vacuum (200 mTorr), followed by slow cooling to room temperature. Vertical lines represent theoretical reflections of the given crystal system as calculated based on the experimental q^* .

patterns: one as-synthesized ABC triblock and two different fractions. The parent sample, while ordered, cannot be assigned a definitive morphology. In contrast, the fraction with $f_L = 26\%$, $f_D = 52\%$, and $f_F = 22\%$ has exceptional long-range hexagonal ordering as evidenced by q reflections up to $\sqrt{49} q^*$, where q is the magnitude of the scattering wave vector ($q = |\mathbf{q}|$) and $q^* = 2\pi/d_{10}$ corresponds with the $\{10\}$ family of planes in the hexagonal plane group $p6mm$ having interplanar spacing d_{10} . From the same starting parent terpolymer, another fraction with $f_L = 18\%$, $f_D = 50\%$, and $f_F = 32\%$ shows excellent agreement between the actual peak positions and those calculated for a cubic crystal system up to $\sqrt{38} q^*$, where $q^* = 2\pi/d_{100}$ is the magnitude of the $\{100\}$ family of planes with interplanar spacing d_{100} . Note that there are also small peaks at $\sqrt{7} q^*$ and $\sim\sqrt{15} q^*$, which are not allowed in cubic crystals, suggesting a minor amount of coexisting HEX with similar q^* (Figure S22). This sample is labeled “cubic” rather than specifying a particular unit cell structure as we were unable to definitively distinguish between core–shell and alternating spheres from hard X-ray scattering alone. However, we speculate that this triblock terpolymer exhibits an alternating spherical structure (space group $Pm\bar{3}m$, #221)

based on a simple cubic crystal due to no apparent restrictions on the observed values of (hkl) that would otherwise arise in more symmetric morphologies (e.g., core–shell spheres with space group $Im\bar{3}m$, #229). The common origin of these fractions from the same ill-defined parent triblock (LDF-22) demonstrates the power of chromatography in analyzing phase behavior. Additionally, the large number of reflections observed with these materials is notable compared with prior studies on traditional, non-fractionated triblock terpolymers. For example, Noda reported cylindrical and spherical morphologies of an ABC triblock terpolymer poly(isoprene)-block-poly(styrene)-block-poly(2-vinylpyridine) having only two and three reflections, respectively, by SAXS, which is in contrast to the >20 reflections observed here.⁴⁷

To further demonstrate the utility of combining orthogonal controlled polymerizations with automated chromatography for accelerating discovery of nanostructures within ternary phase space, we next synthesized four additional poly(4-methyl caprolactone)-block-poly(dodecyl acrylate)-block-poly(2,2,2-trifluoroethyl acrylate) samples (LDF-19, LDF-43, LDF-18, and LDF-17) (Table S1). These parent triblock terpolymers were designed to each occupy a unique position in the phase diagram with significant differences in composition but comparable overall molecular weights $\langle M_n \rangle = 42–51$ kDa and dispersities $\langle D \rangle = 1.06–1.15$ (Figure 5a). The synthetic

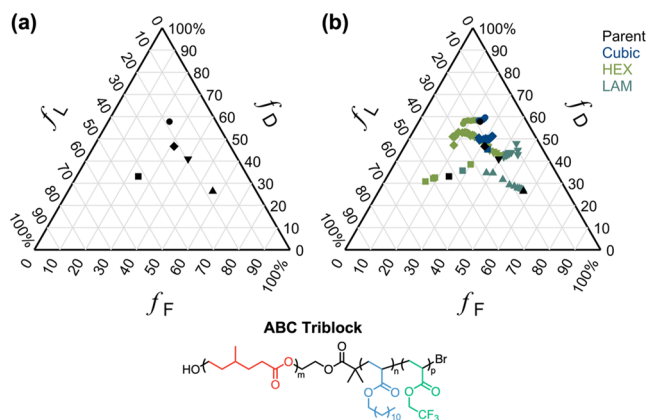


Figure 5. (a) Composition of five as-synthesized, parent ABC triblock terpolymers. (b) Library of 87 well-defined, fractionated ABC triblock terpolymers generated via automated chromatography. Fractionated terpolymers are depicted with the same shape as their respective parent material.

approach, starting from an orthogonal difunctional initiator, was the same for all parent terpolymers with conditions for fractionation being analogous to LDF-22 as described above. This diversity in initial parent terpolymer structures provided an extensive library of purified ABC triblock terpolymers with a wide range of compositions from only five parent materials (Figure S17). Separations were readily scaled to greater than 1.5 g by simply using a larger column cartridge with the same optimized solvent gradient. It should also be noted that in prior experimental and theoretical studies, ABC triblock terpolymer phase diagrams were shown to be significantly impacted by the presence of homopolymer and diblock copolymer impurities,^{48,49} adding additional complexity to understanding the relationship between polymer structure and nanoscale morphology. The ability of fractionation to generate polymer libraries and also remove homopolymer/diblock

copolymer impurities is an important advantage for multi-step controlled polymerization procedures, which leads to improved reproducibility (Figure S17).

Figure 5b summarizes the different well-defined morphologies found for these fractionated ABC terpolymers. As clearly illustrated by SAXS analysis of multiple samples, cubic and HEX regions were observed in the ternary phase diagram at higher volume percentages of poly(dodecyl acrylate), whereas F-rich materials led to lamellar (LAM) morphologies. In contrast, only one of the five parent ABC triblock copolymers displayed a well-defined morphology (LAM), with distinct differences being noted between parent and fractionated samples of similar molecular weights and volume fractions. For example, a fractionated sample of LDF-43 was obtained with $f_L = 22\%$, $f_D = 45\%$, and $f_F = 33\%$ assembled into a well-defined cubic morphology (Figure S24). In contrast, the parent LDF-22 terpolymer with a similar composition $\langle f_L \rangle = 22\%$, $\langle f_D \rangle = 47\%$, and $\langle f_F \rangle = 31\%$ remained ill-defined even after extended thermal annealing (Figure 4). This difference underscores the ability of automated chromatography to generate block copolymer samples with increased purity and long-range order when compared to as-synthesized materials. In addition, obtaining over 80 fractionated ABC triblock terpolymers from just five parent triblocks illustrates the significant acceleration in discovery that is afforded by this combination of controlled polymerization and automated chromatography (Figure 5b).

The versatility of our synthetic strategy also provides facile access to the isomeric ACB terpolymer sequence: poly(4-methyl caprolactone)-block-poly(2,2,2-trifluoroethyl acrylate)-block-poly(dodecyl acrylate). In this case, the same poly(4-methyl caprolactone) homopolymer starting material was sequentially chain-extended in the reverse order with initial growth of a poly(2,2,2-trifluoroethyl acrylate) block followed by poly(dodecyl acrylate), again under photo-ATRP conditions. As with the ABC derivatives, good end-group retention led to well-defined ACB triblock terpolymers in high yields. These isomeric parent materials (labeled LFD-41, LFD-19, and LFD-17) were synthesized with similar molar masses and volume fractions as the corresponding ABC sequence (Figure 6a, Table S8). This type of subtle change in block connectivity, from ABC to ACB, is well known to influence self-assembly as the pattern of interfacial tension changes (so-called “frus-

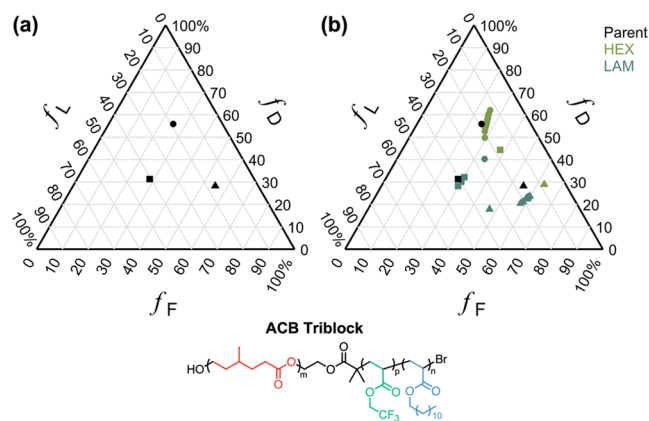


Figure 6. (a) Composition of three as-synthesized parent ACB triblock terpolymers. (b) Library of 25 well-defined fractions obtained by automated chromatography. Fractionated terpolymers are depicted with the same shape as their respective parent material.

tration”).^{9,10,50} ACB triblock terpolymers were fractionated using similar solvent gradients to the analogous ABC isomers, resulting in a library of well-defined terpolymer samples with high mass recovery (>80%) (Figure S35). Notably, fractionation of the ACB terpolymers also afforded consistent changes in composition as a function of fraction number, with a linear increase in f_L and decrease in f_F for all three parent terpolymers (Figure S35). As shown in Figure 6b, a detailed phase diagram was obtained, highlighting different regions of HEX and LAM stability. In agreement with our results for the ABC sequence, significant long-range order up to $\sqrt{75} q^*$ and $10q^*$ was observed for HEX and LAM, respectively (Figure 7).

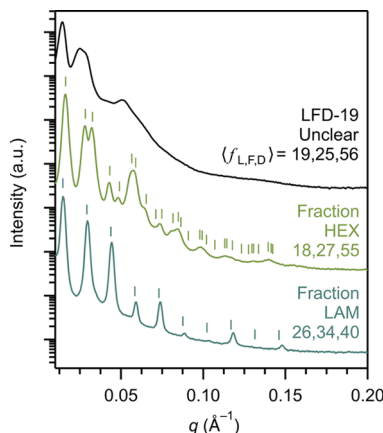


Figure 7. Selected SAXS profiles of the topological ACB triblock terpolymer isomer (LFD-19) and fractionated samples derived therefrom. All SAXS experiments were conducted at room temperature. Triblock terpolymers were annealed at 130 °C for 15 h and then 70 °C for 24 h under vacuum (200 mTorr), followed by slow cooling to room temperature. Vertical lines represent theoretical reflections of the given crystal system as calculated based on the experimental q^* .

This is in contrast to less-defined morphologies observed for parent ACB terpolymers as illustrated with LFD-19. Collectively, these results demonstrate that automated chromatography is equally effective at separating block copolymers with the same chemistry but different sequences (e.g., ABC and ACB), where 25 well-ordered fractions were obtained from only three ACB parent triblocks. The versatility of this separation method creates opportunities for future studies to examine the role of block sequence in controlling multi-block copolymer nanostructures.

CONCLUSIONS

The combination of controlled polymerizations with automated chromatographic fractionation is a powerful strategy for mapping the phase behavior of complex ABC triblock terpolymers. From a single difunctional initiator, both ABC and ACB triblock libraries together containing over 100 fractionated samples were prepared from a small number (<10) of parent terpolymers. This general technique dramatically accelerates the experimental study of triblock terpolymer morphologies across a large parameter space. Compared to conventional methods involving serial syntheses of individual triblock terpolymers, chromatographic fractionation is simple, scalable, and leads to increased reproducibility through the efficient removal of homopolymer and diblock copolymer impurities. One consequence is a significant

increase in long-range order for samples purified by automated chromatography as highlighted by differences between parent and fractionated terpolymers. These studies demonstrate the synergy between automated chromatography and controlled polymerization procedures in the development of user-friendly strategies for accelerating the study of structure–property relationships in multi-block polymers with increasingly complex architectures and well-defined monomer sequences. This enhanced discovery process is critical to support the greater range of block copolymer possibilities enabled by advances in controlled polymerizations.

ASSOCIATED CONTENT

Supporting Information

The Supporting Information is available free of charge at <https://pubs.acs.org/doi/10.1021/acs.macromol.2c01480>. Data used in all figures throughout the main text and Supporting Information are also available free of charge at 10.25349/D9NG89.

Experimental procedures and characterization data for block copolymers, including ^1H NMR, SEC, differential scanning calorimetry, matrix-assisted laser desorption/ionization mass spectrometry, optimization of fractionation conditions, fractionation of ABC triblock terpolymers, fractionation of ACB triblock terpolymers, and SAXS (PDF)

AUTHOR INFORMATION

Corresponding Authors

Morgan W. Bates — Materials Research Laboratory, University of California, Santa Barbara, California 93106, United States; orcid.org/0000-0002-8939-2682; Email: morganbates@mrl.ucsb.edu

Cheng Zhang — Materials Research Laboratory, University of California, Santa Barbara, California 93106, United States; Australian Institute for Bioengineering and Nanotechnology, University of Queensland, Brisbane, Queensland 4072, Australia; orcid.org/0000-0002-2722-7497; Email: c.zhang3@uq.edu.au

Christopher M. Bates — Materials Research Laboratory, Department of Chemistry & Biochemistry, Department of Chemical Engineering, and Materials Department, University of California, Santa Barbara, California 93106, United States; orcid.org/0000-0002-1598-794X; Email: cbates@ucsb.edu

Craig J. Hawker — Materials Research Laboratory, Department of Chemistry & Biochemistry, and Materials Department, University of California, Santa Barbara, California 93106, United States; orcid.org/0000-0001-9951-851X; Email: hawker@mrl.ucsb.edu

Authors

Elizabeth A. Murphy — Materials Research Laboratory and Department of Chemistry & Biochemistry, University of California, Santa Barbara, California 93106, United States; orcid.org/0000-0003-0846-7943

Yan-Qiao Chen — Materials Research Laboratory, University of California, Santa Barbara, California 93106, United States

Kaitlin Albanese — Materials Research Laboratory and Department of Chemistry & Biochemistry, University of California, Santa Barbara, California 93106, United States

Jacob R. Blankenship – Materials Research Laboratory and Department of Chemistry & Biochemistry, University of California, Santa Barbara, California 93106, United States

Allison Abdilla – Materials Research Laboratory and Department of Chemistry & Biochemistry, University of California, Santa Barbara, California 93106, United States

Complete contact information is available at:
<https://pubs.acs.org/10.1021/acs.macromol.2c01480>

Author Contributions

The manuscript was written by E.A.M., Y-Q.C., M.W.B., C.Z., C.M.B., and C.J.H. Experiments were designed by E.A.M., Y-Q.C., K.A., A.A., M.W.B., C.Z., C.M.B., and C.J.H. and performed by E.A.M., Y-Q.C., K.A., and J.R.B. All authors have given approval to the final version of the manuscript.

Funding

The research reported here was primarily supported by the National Science Foundation Materials Research Science and Engineering Center (MRSEC) at UC Santa Barbara (DMR-1720256, IRG-3, C.M.B. and C.J.H., synthesis), DMR-1844987 (C.M.B., characterization), and the BioPACIFIC Materials Innovation Platform of the National Science Foundation under Award No. DMR-1933487 (C.M.B., C.J.H., equipment and characterization). The research reported here made use of shared facilities of the UC Santa Barbara MRSEC (NSF DMR-1720256), a member of the Materials Research Facilities Network (www.mrfn.org). E.A.M. gratefully acknowledges the National Science Foundation Graduate Research Fellowship Program under grant 2139319. A.A. thanks the Natural Sciences and Engineering Council of Canada (NSERC) for financial support. C.Z. acknowledges support from the National Health and Medical Research Council for an Early Career Fellowship (APP1157440).

Notes

The authors declare no competing financial interest.

■ REFERENCES

- (1) Bates, C. M.; Bates, F. S. 50th Anniversary Perspective: Block Polymers—Pure Potential. *Macromolecules* **2017**, *50*, 3–22.
- (2) Mai, Y.; Eisenberg, A. Self-Assembly of Block Copolymers. *Chem. Soc. Rev.* **2012**, *41*, 5969–5985.
- (3) Cabral, H.; Miyata, K.; Osada, K.; Kataoka, K. Block Copolymer Micelles in Nanomedicine Applications. *Chem. Rev.* **2018**, *118*, 6844–6892.
- (4) Bates, M.; Janes, J.; Willson, W.; Ellison, J.; Grant, W.; Block, C. Block Copolymer Lithography. *Macromolecules* **2014**, *47*, 2–12.
- (5) Bates, F. S.; Fredrickson, G. H. Block Copolymers—Designer Soft Materials. *Phys. Today* **1999**, *52*, 32–38.
- (6) Matsen, M. W.; Bates, F. S. Origins of Complex Self-Assembly in Block Copolymers. *Macromolecules* **1996**, *29*, 7641–7644.
- (7) Matsen, M. W. Field Theoretic Approach for Block Polymer Melts: SCFT and FTS. *J. Chem. Phys.* **2020**, *152*, 5098.
- (8) Bates, F. S.; Hillmyer, M. a.; Lodge, T. P.; Bates, C. M.; Delaney, K. T.; Fredrickson, G. H. Multiblock Polymers: Panacea or Pandora's Box? *Science* **2012**, *336*, 434–440.
- (9) Hückstädt, H.; Göpfert, A.; Abetz, V. Influence of the Block Sequence on the Morphological Behavior of ABC Triblock Copolymers. *Polymer* **2000**, *41*, 9089–9094.
- (10) Chen, Z.; Cui, H.; Hales, K.; Li, Z.; Qi, K.; Pochan, D. J.; Wooley, K. L. Unique Toroidal Morphology from Composition and Sequence Control of Triblock Copolymers. *J. Am. Chem. Soc.* **2005**, *127*, 8592–8593.
- (11) Jiang, Y.; Yan, X.; Liang, H.; Shi, A. C. Effect of Polydispersity on the Phase Diagrams of Linear ABC Triblock Copolymers in Two Dimensions. *J. Phys. Chem. B* **2005**, *109*, 21047–21055.
- (12) Antonopoulou, M. N.; Whitfield, R.; Truong, N. P.; Wyers, D.; Harrisson, S.; Junkers, T.; Anastasaki, A. Concurrent Control over Sequence and Dispersity in Multiblock Copolymers. *Nat. Chem.* **2022**, *14*, 304–312.
- (13) Engelis, N. G.; Anastasaki, A.; Nurumbetov, G.; Truong, N. P.; Nikolaou, V.; Shegiwal, A.; Whittaker, M. R.; Davis, T. P.; Haddleton, D. M. Sequence-Controlled Methacrylic Multiblock Copolymers via Sulfur-Free RAFT Emulsion Polymerization. *Nat. Chem.* **2017**, *9*, 171–178.
- (14) Engelis, N. G.; Anastasaki, A.; Whitfield, R.; Jones, G. R.; Liarou, E.; Nikolaou, V.; Nurumbetov, G.; Haddleton, D. M. Sequence-Controlled Methacrylic Multiblock Copolymers: Expanding the Scope of Sulfur-Free RAFT. *Macromolecules* **2018**, *51*, 336–342.
- (15) Anastasaki, A.; Oschmann, B.; Willenbacher, J.; Melker, A.; Van Son, M. H. C.; Truong, N. P.; Schulze, M. W.; Discekici, E. H.; McGrath, A. J.; Davis, T. P.; Bates, C. M.; Hawker, C. J. One-Pot Synthesis of ABCDE Multiblock Copolymers with Hydrophobic, Hydrophilic, and Semi-Fluorinated Segments. *Angew. Chem., Int. Ed.* **2017**, *56*, 14483–14487.
- (16) Zhang, C.; Bates, M. W.; Geng, Z.; Levi, A. E.; Vigil, D.; Barbon, S. M.; Loman, T.; Delaney, K. T.; Fredrickson, G. H.; Bates, C. M.; Whittaker, A. K.; Hawker, C. J. Rapid Generation of Block Copolymer Libraries Using Automated Chromatographic Separation. *J. Am. Chem. Soc.* **2020**, *142*, 9843–9849.
- (17) Zhang, C.; Vigil, D. L.; Sun, D.; Bates, M. W.; Loman, T.; Murphy, E. A.; Barbon, S. M.; Song, J. A.; Yu, B.; Fredrickson, G. H.; Whittaker, A. K.; Hawker, C. J.; Bates, C. M. Emergence of Hexagonally Close-Packed Spheres in Linear Block Copolymer Melts. *J. Am. Chem. Soc.* **2021**, *143*, 14106–14114.
- (18) Lawrence, J.; Lee, S. H.; Abdilla, A.; Nothling, M. D.; Ren, J. M.; Knight, A. S.; Fleischmann, C.; Li, Y.; Abrams, A. S.; Schmidt, B. V. K. J.; Hawker, M. C.; Connal, L. A.; McGrath, A. J.; Clark, P. G.; Gutekunst, W. R.; Hawker, C. J. A Versatile and Scalable Strategy to Discrete Oligomers. *J. Am. Chem. Soc.* **2016**, *138*, 6306–6310.
- (19) Lawrence, J.; Goto, E.; Ren, J. M.; McDearmon, B.; Kim, D. S.; Ochiai, Y.; Clark, P. G.; Laitar, D.; Higashihara, T.; Hawker, C. J. A Versatile and Efficient Strategy to Discrete Conjugated Oligomers. *J. Am. Chem. Soc.* **2017**, *139*, 13735–13739.
- (20) Haven, J. J.; De Neve, J.; Castro Villavicencio, A.; Junkers, T. Elucidation of the Properties of Discrete Oligo(Meth)Acrylates. *Polym. Chem.* **2019**, *10*, 6540–6544.
- (21) Haven, J. J.; Junkers, T. Quasi-Monodisperse Polymer Libraries Via Flash Column Chromatography: Correlating Dispersity with Glass Transition. *Polym. Chem.* **2019**, *10*, 679–682.
- (22) Báez, J. E.; Shea, K. J.; Dennison, P. R.; Obregón-Herrera, A.; Bonilla-Cruz, J. Monodisperse Oligo(δ -Valerolactones) and Oligo(ϵ -Caprolactones) with Docosyl (C_{22}) End-Groups. *Polym. Chem.* **2020**, *11*, 4228–4236.
- (23) Hoshino, Y.; Taniguchi, S.; Takimoto, H.; Akashi, S.; Katakami, S.; Yonamine, Y.; Miura, Y. Homogeneous Oligomeric Ligands Prepared via Radical Polymerization That Recognize and Neutralize a Target Peptide. *Angew. Chem., Int. Ed.* **2020**, *59*, 679–683.
- (24) Maes, L.; Massana Roqueiro, D.; Pitet, L. M.; Adriaensens, P.; Junkers, T. Sequence-Defined Nucleobase Containing Oligomers: Via Reversible Addition-Fragmentation Chain Transfer Single Monomer Addition. *Polym. Chem.* **2020**, *11*, 2027–2033.
- (25) Shi, X.; Liu, M.; Li, L.; Zhang, J.; Li, H.; Huang, Z.; Zhang, W.; Zhang, Z.; Zhou, N.; Zhu, X. Efficient Synthesis of Discrete Oligo(Fluorenediacylene)s toward Chain-Length-Dependent Optical and Structural Properties. *Polym. Chem.* **2021**, *12*, 2598–2605.
- (26) Ogbonna, N. D.; Dearman, M.; Cho, C. T.; Bharti, B.; Peters, A. J.; Lawrence, J. Topologically Precise and Discrete Bottlebrush Polymers: Synthesis, Characterization, and Structure-Property Relationships. *J. Am. Chem. Soc.* **2022**, *2*, 898–905.
- (27) Romio, M.; Grob, B.; Trachsel, L.; Mattarei, A.; Morgese, G.; Ramakrishna, S. N.; Niccolai, F.; Guazzelli, E.; Paradisi, C.; Martinelli,

- E.; Spencer, N. D.; Benetti, E. M. Dispersion within Brushes Plays a Major Role in Determining Their Interfacial Properties: The Case of Oligoxazoline-Based Graft Polymers. *J. Am. Chem. Soc.* **2021**, *143*, 19067–19077.
- (28) Ren, J. M.; Lawrence, J.; Knight, A. S.; Abdilla, A.; Zerdan, R. B.; Levi, A. E.; Oschmann, B.; Gutekunst, W. R.; Lee, S. H.; Li, Y.; McGrath, A. J.; Bates, C. M.; Qiao, G. G.; Hawker, C. J. Controlled Formation and Binding Selectivity of Discrete Oligo(Methyl Methacrylate) Stereocomplexes. *J. Am. Chem. Soc.* **2018**, *140*, 1945–1951.
- (29) Oschmann, B.; Lawrence, J.; Schulze, M. W.; Ren, J. M.; Anastasaki, A.; Luo, Y.; Nothling, M. D.; Pester, C. W.; Delaney, K. T.; Connal, L. A.; McGrath, A. J.; Clark, P. G.; Bates, C. M.; Hawker, C. J. Effects of Tailored Dispersion on the Self-Assembly of Dimethylsiloxane–Methyl Methacrylate Block Co-Oligomers. *ACS Macro Lett.* **2017**, *6*, 668–673.
- (30) Zhang, C.; Kim, D. S.; Lawrence, J.; Hawker, C. J.; Whittaker, A. K. Elucidating the Impact of Molecular Structure on the ¹⁹F NMR Dynamics and MRI Performance of Fluorinated Oligomers. *ACS Macro Lett.* **2018**, *7*, 921–926.
- (31) Kim, Y.; Park, H.; Abdilla, A.; Yun, H.; Han, J.; Stein, G. E.; Hawker, C. J.; Kim, B. J. Chain-Length-Dependent Self-Assembly Behaviors of Discrete Conjugated Oligo(3-Hexylthiophene). *Chem. Mater.* **2020**, *32*, 3597–3607.
- (32) Haven, J. J.; De Neve, J. A.; Junkers, T. Versatile Approach for the Synthesis of Sequence-Defined Monodisperse 18- and 20-Mer Oligoacrylates. *ACS Macro Lett.* **2017**, *6*, 743–747.
- (33) Vail, N. S.; Stubbs, C.; Biggs, C. I.; Gibson, M. I. Ultralow Dispersion Poly(Vinyl Alcohol) Reveals Significant Dispersion Effects on Ice Recrystallization Inhibition Activity. *ACS Macro Lett.* **2017**, *6*, 1001–1004.
- (34) Das, A.; Petkau-Milroy, K.; Klerks, G.; van Genabeek, B.; Lafleur, R. P. M.; Palmans, A. R. A.; Meijer, E. W. Consequences of Dispersion on the Self-Assembly of ABA-Type Amphiphilic Block Co-Oligomers. *ACS Macro Lett.* **2018**, *7*, 546–550.
- (35) De Neve, J.; Haven, J. J.; Harrisson, S.; Junkers, V.; Deconstructing, T. Oligomer Distributions: Discrete Species and Artificial Distributions. *Angew. Chem., Int. Ed.* **2019**, *131*, 14007–14011.
- (36) Ponyik, C. A.; Wu, D. T.; Williams, S. K. R. Separation and Composition Distribution Determination of Triblock Copolymers by Thermal Field-Flow Fractionation. *Anal. Bioanal. Chem.* **2013**, *405*, 9033–9040.
- (37) Epps, T. H.; Cochran, E. W.; Bailey, T. S.; Waletzko, R. S.; Hardy, C. M.; Bates, F. S. Ordered Network Phases in Linear Poly(Isoprene-*b*-Styrene-*b*-Ethylene Oxide) Triblock Copolymers. *Macromolecules* **2004**, *37*, 8325–8341.
- (38) Epps, T. H.; Cochran, E. W.; Hardy, C. M.; Bailey, T. S.; Waletzko, R. S.; Bates, F. S. Network Phases in ABC Triblock Copolymers. *Macromolecules* **2004**, *37*, 7085–7088.
- (39) Epps, T. H.; Bates, F. S. Effect of Molecular Weight on Network Formation in Linear ABC Triblock Copolymers. *Macromolecules* **2006**, *39*, 2676–2682.
- (40) Hückstädt, H.; Goldacker, T.; Göpfert, A.; Abetz, V. Core–Shell Double Gyroid Morphologies in ABC Triblock Copolymers. *Macromolecules* **2000**, *33*, 3757–3761.
- (41) Gil Haenelt, T.; Meyer, A.; Abetz, C.; Abetz, V. Planet-Like Nanostructures Formed by an ABC Triblock Terpolymer. *Macromol. Chem. Phys.* **2019**, *220*, 1900297.
- (42) Breiner, U.; Krappe, U.; Abetz, V.; Stadler, R. Cylindrical Morphologies in Asymmetric ABC Triblock Copolymers. *Macromol. Chem. Phys.* **1997**, *198*, 1051–1083.
- (43) Barbon, S. M.; Song, J. A.; Chen, D.; Zhang, C.; Lequieu, J.; Delaney, K. T.; Anastasaki, A.; Rolland, M.; Fredrickson, G. H.; Bates, M. W.; Hawker, C. M.; Bates, C. J. Architecture Effects in Complex Spherical Assemblies of (AB)_n-Type Block Copolymers. *ACS Macro Lett.* **2020**, *9*, 1745–1752.
- (44) Watts, A.; Kurokawa, N.; Hillmyer, M. A. Strong, Resilient, and Sustainable Aliphatic Polyester Thermoplastic Elastomers. *Biomacromolecules* **2017**, *18*, 1845–1854.
- (45) Barbon, S. M.; Rolland, M.; Anastasaki, A.; Truong, N. P.; Schulze, M. W.; Bates, C. M.; Hawker, C. J. Macrocyclic Side-Chain Monomers for Photoinduced ATRP: Synthesis and Properties versus Long-Chain Linear Isomers. *Macromolecules* **2018**, *51*, 6901–6910.
- (46) Discekici, E. H.; Anastasaki, A.; Kaminker, R.; Willenbacher, J.; Truong, N. P.; Fleischmann, C.; Oschmann, B.; Lunn, D. J.; Read de Alaniz, J.; Davis, T. P.; Bates, C. M.; Hawker, C. J. Light-Mediated Atom Transfer Radical Polymerization of Semi-Fluorinated (Meth)Acrylates: Facile Access to Functional Materials. *J. Am. Chem. Soc.* **2017**, *139*, 5939–5945.
- (47) Mogi, Y.; Nomura, M.; Kotsuji, H.; Ohnishi, K.; Matsushita, Y.; Noda, I. Superlattice Structures in Morphologies of the ABC Triblock Copolymers. *Macromolecules* **1994**, *27*, 6755–6760.
- (48) Chen, K.; Wang, F.; Liu, M.; Wang, X. Tunable Helical Structures Formed by Blending ABC Triblock Copolymers and C Homopolymers in Nanopores. *Polym. Int.* **2022**, *71*, 444–450.
- (49) Wickham, R. A.; Shi, A. C. Noncentrosymmetric Lamellar Phase in Blends of ABC Triblock and AC Diblock Copolymers. *Macromolecules* **2001**, *34*, 6487–6494.
- (50) Chang, A. B.; Bates, F. S. The ABCs of Block Polymers. *Macromolecules* **2020**, *53*, 2765–2768.